Biofilm 2 (2020) 100023

Contents lists available at ScienceDirect

Biofilm

journal homepage: www.elsevier.com/locate/bioflm

Genetic determinants of *Pseudomonas aeruginosa* fitness during biofilm growth

Silvia Schinner [a], Florian Engelhardt [a], Matthias Preusse [a], Janne Gesine Thöming [b,c], Jürgen Tomasch [a], Susanne Häussler [a,b,c,d,*]

[a] Department of Molecular Bacteriology, Helmholtz Centre for Infection Research, Braunschweig, Germany
[b] Institute of Molecular Bacteriology, TWINCORE Centre for Experimental and Clinical Infection Research, Hannover, Germany
[c] Department of Clinical Microbiology, Copenhagen University Hospital – Rigshospitalet, Copenhagen, Denmark
[d] Cluster of Excellence RESIST (EXC 2155), Hannover Medical School, Hannover, Germany

ARTICLE INFO

Keywords:
Tn-seq
Pseudomonas aeruginosa
Biofilm
Fitness determinants

ABSTRACT

Pseudomonas aeruginosa is an environmental bacterium and an opportunistic human pathogen. It is also a well-established model organism to study bacterial adaptation to stressful conditions, such as those encountered during an infection process in the human host. Advancing knowledge on *P. aeruginosa* adaptation to biofilm growth conditions is bound to reveal novel strategies and targets for the treatment of chronic biofilm-associated infections. Here, we generated transposon insertion libraries in three *P. aeruginosa* strain backgrounds and determined the relative frequency of each insertion following biofilm growth using transposon sequencing. We demonstrate that in general the SOS response, several tRNA modifying enzymes as well as adaptation to microaerophilic growth conditions play a key role in bacterial survival under biofilm growth conditions. On the other hand, presence of genes involved in motility and PQS signaling were less important during biofilm growth. Several mutants exhibiting transposon insertions in genes detected in our screen were validated for their biofilm growth capabilities and biofilm specific transcriptional responses using independently generated transposon mutants. Our results provide new insights into *P. aeruginosa* adaptation to biofilm growth conditions. The detection of previously unknown determinants of biofilm survival supports the use of transposon insertion sequencing as a global genomic technology for understanding the establishment of difficult to treat biofilm-associated infections.

Introduction

Bacteria in biofilms are protected by self-produced extracellular matrices and exhibit an increased resistance to a wide range of adverse conditions [1–3]. In the human host, biofilm-associated bacteria are responsible for persistent infections [4–6]. These infections affect millions of people and are a leading cause of death and disability. With progress in medical sciences, more and more indwelling devices for the purpose of medical treatments and foreign body implants are applied. Biofilm-associated infections continue to be a major complication of their use. There are also severe biofilm-associated infections, which are not associated with foreign bodies, such as chronic wound infections, infections of the middle ear and of the lungs of cystic fibrosis patients. Many of those infections are caused by the opportunistic pathogen *Pseudomonas aeruginosa* [7]. Once a *P. aeruginosa* biofilm-associated infection is established, it withstands antibiotic treatment and the host immune response, and it becomes almost impossible to eradicate. Thus, new knowledge on etiological mechanisms underlying the establishment of biofilms and the evolution of biofilm resistance is essential in order to meet the urgent medical need for new therapy options. Identification of the set of genes that are required for biofilm establishment and biofilm-associated tolerance might lead to new targets that could become the basis for the development of novel anti-biofilm therapies.

The role of individual genes in defining distinct phenotypes is usually assessed by measuring the fitness of respective mutants in habitats, where the phenotype is expressed. Recently, global genomics-based approaches termed transposon directed insertion-site sequencing (TraDIS [8,9]) or transposon sequencing (Tn-seq [10]) have very successfully been used to identify genes involved in the expression of distinct phenotypes, such as resistance and persister cell formation [11,12],

* Corresponding author. Department of Molecular Bacteriology, Helmholtz Centre for Infection Research, Braunschweig, Germany.
E-mail address: susanne.haeussler@helmholtz-hzi.de (S. Häussler).

https://doi.org/10.1016/j.bioflm.2020.100023
Received 16 November 2019; Received in revised form 19 March 2020; Accepted 20 March 2020
Available online 2 April 2020

pathogenicity [13,14], twitching induced biofilm expansion [15], or bacterial adaptation to stress conditions [16,17]. These global approaches involve tracking of the relative frequency of transposon insertions in input pools of mutant libraries compared to output pools after growth in the selective conditions using deep sequencing [18].

In this study, the comparison of three different *P. aeruginosa* isolate input and output mutant pools led to the identification of genes that positively and negatively contribute to survival under biofilm growth conditions. Our results imply that there is a common theme of *P. aeruginosa* adaptation to these conditions. To substantiate the role of individual *P. aeruginosa* genes in biofilm formation, we determined the transcriptional response of the *P. aeruginosa* wild-types as well as selected mutants under biofilm growth conditions. Our results demonstrate the value of functional genomics approaches to study bacterial strategies responsible for chronic, biofilm-associated infections and highlight their potential to uncover unexpected functional gene categories that are involved in biofilm formation and maintenance.

Material and methods

Bacterial strains and growth conditions

All bacterial strains and primers used in this study are listed in Supplementary Table S1. Seven Tn mutants were selected from the non-redundant set of transposon mutants derived from PA14 (PA14NR) described by Liberati et al. (2006) [19]. Tn*ladS* served as a wild-type control for the Tn mutants. The *ladS* gene is not active in the PA14 strain background. Thus, the Tn insertion into the *ladS* gene provides the strain with a transposon without functional consequences. All bacterial strains were cultivated in lysogeny broth (LB; 1 l = 5 g yeast extract, 7.5 g NaCl, 10 g tryptone) at 37 °C unless otherwise stated. LB agar contained 1.6% (w/v) bactoagar. Biofilms were cultivated under static conditions in a humid atmosphere. Planktonic cultures were incubated in an orbital shaker (180 rpm). Growth curves of bacterial strains were recorded by monitoring the optical density at 600 nm (OD_{600}) using a SYNERGY H1 microplate reader (BioTek). In brief, overnight cultures were diluted to OD_{600} = 0.05 and 200 µl cultures were grown at 37 °C under shaking conditions in the wells of a Nunc™ MicroWell™ 96-Well Microplate (Nunclon Delta). OD_{600} values were recorded for two biological replicates (each in technical triplicates) every 15 min for a time period of 24 h.

P. aeruginosa Tn mutagenesis

Tn mutagenesis was carried out by conjugation of the *P. aeruginosa* acceptor strain with donor *E. coli* β2155 λpir harboring pBT20, which encodes the mariner Himar1 C9 transposon, followed by selection for *P. aeruginosa* cells harboring the Tn-containing gentamicin-resistance on selective agar plates [20]. *E. coli* β2155 λpir harbors a Δ*dapA* mutation, resulting in a diaminopimelic acid (DAP) auxotrophic phenotype, which facilitates post-conjugational counterselection. In brief, donor *E. coli* β2155 λpir [pBT20] was cultivated overnight at 37 °C on 0.3 mM DAP and ampicillin (100 µg/ml)-containing LB plates and the acceptor *P. aeruginosa* at 42 °C on LB plates. For conjugation, strains were mixed at a 1:1 ratio and incubated for 2 h at 37 °C on 0.3 mM DAP-containing LB plates. Conjugation mixtures were plated on selective Vogel–Bonner–Minimal (VBM) agar supplemented with gentamicin (200 µg/ml) and grown overnight at 37 °C [20]. *P. aeruginosa* Tn mutants were harvested, glycerol stocks prepared and stored at −80 °C [13]. 5.07×10^5 colony forming units (CFU), 1.90×10^6 CFU and 4.61×10^5 CFU, were pooled to generate the Tn mutant libraries of PA14, PAO1 and ZG8038581181, respectively. The PA14 genome consists of 100,391 TA sites, thus a Tn mutant library consisting of $> 4.00 \times 10^5$ CFU is expected to be > 98% saturated.

Confocal microscopy to record biofilm phenotypes

Biofilm phenotypes were monitored using a high-throughput static microtiter plate assay combined with automated confocal laser scanning microscopy. As previously described [21], bacteria were grown overnight in LB at 37 °C and 100 µl of bacterial suspension with an adjusted OD_{600} of 0.002 were added to the wells of a sterile half-area 96-well µClear microtiter plate (Greiner Bio-One). The microtiter plate was sealed with an air-permeable BREATHseal cover foil (Greiner Bio-One) and incubated for 48 h in humid atmosphere at 37 °C under static conditions. After 24 h, bacteria were stained by carefully adding 60 µl of a solution containing the fluorescent dyes Syto9 and propidium iodide (final concentrations of 2.1 µM and 12.5 µM, respectively) from the LIVE/DEAD® BacLight™ Bacterial Viability Kit (Molecular Probes, Life Technologies). Z-Stacks of 48 h-old biofilms with a total height of 60 µm (20 focal planes; z-step size 3 µm) in the centre of each well were acquired by using an automated confocal laser scanning microscope (SP8 System, Leica) including the matrix screener tool and equipped with an HC PL APO 40x/1.10 W motCORR CS2 water immersion objective. For biofilm quantification, acquired image stacks were analyzed as previously described [21] with slight modifications. In brief, the customized software Definiens Developer XD was used to determine the biofilm biovolume, which describes the biomass. Images were analyzed with an automated thresholding and the minimum biofilm size was defined as 4 μm^2. The biofilm phenotype was recorded for all strains in triplicates. For 3D reconstructions of biofilm structures the sectioning mode of Imaris 7.6 (Bitplane, UK) was used.

Growth of Tn mutant libraries under biofilm conditions

Tn mutant libraries were grown in biofilms in a 96-well format using a high-throughput static microtiter plate assay as described in the previous section. In brief, Tn mutant libraries were inoculated directly from glycerol stock in LB and 100 µl of bacterial suspension with an adjusted OD_{600} of 0.002 were added to the wells (12 wells per sample) of a sterile half-area 96-well µClear microtiter plate. 100 µl of the glycerol stock was sequenced as the input sample. For the biofilm assay, the microtiter plate was sealed with an air-permeable BREATHseal cover foil and incubated for 48 h in humid atmosphere at 37 °C. After 24 h, 60 µl of a solution containing 20 µl LB with DMSO (1:200) and 40 µl dH_2O were added carefully to each well (to reproduce the conditions under which the biofilm images were taken). Cultures of 12 (whole) wells per sample were pooled and treated with propidium monoazide (PMA) according to manufacturer's instruction (Biotium). PMA was added at a final concentration of 50 µM, incubated in the dark (5 min, RT and 300 rpm) and exposed to light for 10 min (Intas LED-Illuminator, extinction 470 nm) to inactivate dsDNA stemming from dead cells [22,23]. Cell pellets were used for genomic DNA extraction.

Tn mutant library preparation and sequencing

Sequencing library preparation was performed as previously described for transposon insertion directed sequencing (TraDIS) by Barquist et al. (2016) as well as following the manufacturer's instruction of NEBNext Ultra DNA Library Prep Kit for Illumina. In brief, 2 µg gDNA of transposon mutant pools were sheared to approximately 300 bp-sized fragments (Adaptive Focused Acoustics (AFA) technology, Covaris®, 10% Duty cycle; Intensity 4; 200 Cycles and Time 100 s). DNA fragments were subsequently end-repaired and dA-tailed. A splinkerette adapter was ligated to DNA fragments using TA ligase mastermix. Size selection (400–500 bp) was performed using magnetic beads of Agencourt AMPure® XP-Kit (NEB, Beckman Coulter Life Sciences), following the manufacturer's instruction. Next, fragments were amplified using SplAP5.x primers (8 nt barcode sequence) and the High Fidelity Mastermix within 15 PCR cycles. Samples were purified by magnetic beads without size selection. DNA quality was monitored by Bioanalyzer

(Agilent genomics) and the library was subsequently subjected to Illumina sequencing using HiSeq 2500 in paired-end mode (50 nt) (for PA14 and PAO1) and in single-end mode (50 nt) for ZG8038581181 with customized Read1primer and iPCRtagSeq primers. Primers are listed in Supplementary Table S1. Sequence reads of Tn mutant libraries were preprocessed using cutadapt [24] to remove forward (AGATCGGAAGAGCGGTTCAGCAGGAATGCCGAGACCGATCTC) and reverse (GAGATCGGTCTCGGCATTCCTGCTGAACCGCTCTTCCGATCT) adapters. Remaining reads were mapped to their reference genomes using bowtie2 (default settings) [9]. Reference genomes from NCBI were used for PA14 (NC_008463.1) and PAO1 (NC_002516.2). The reference genome for clinical isolate ZG8038581181 was de-novo-assembled using SPades (1.13.0) [25,26]. Gene prediction was performed using PROKKA version 1.13.7 [27]. All following analyses were performed using the R environment [28]. Only reads that mapped in pairs (specifically for paired-end data) with a mapping quality ≥ 30 (MAPQ) and at least 99.4% TA sites at the corresponding position in the reference genome were used. To reduce the number of genes that were disrupted but still functional (false positives), we did not consider mutants with transposon insertions within the last 10% of the gene [13]. TA reads were normalized using counts per million (cpm) and the weighted trimmed mean of M-values (TMM, edgeR functions calcNormFactors and cpm). To compare disrupted TA sites between the different samples, a TA site was defined to be disrupted with at least 1 TMM normalized read. A gene was defined as dysfunctional if at least 2 different TA sites were disrupted.

Gene depletion and enrichment was calculated using the R package edgeR [29]. Here, genes with at least 2 counts per million (cpm) in at least 2 samples (smallest number of replicates) were used for further analysis. Genes were considered if their enrichment/depletion was significantly (FDR ≤ 0.05) greater than 2-fold (edgeR function glmTreat). Functional enrichment of significant gene sets was done by hypergeometric testing (R function phyper). Functions were considered as significantly enriched with a FDR adjusted p value ≤ 0.05.

DNA-Sequencing data of clinical isolate ZG8038581181 is available at Sequence Read Archive (SRA) under the accession number PRJNA526797 [26]. Raw transposon sequencing data as well as RNA sequencing data have been submitted to the European Nucleotide Archive (ENA) under the accession number PRJEB35203. Venn diagrams were generated using InteractiVenn [30].

RNA sequencing of biofilm cultures

RNA was extracted from bacteria grown under biofilm conditions as described before [31]. Cells from ten (whole) wells per duplicate were pooled and mixed with an equal volume of RNAlater (Qiagen), centrifuged and stored overnight at −80 °C. For RNA extraction, the RNeasy© Mini Kit (Qiagen) in combination with QIAshredder™ columns (Qiagen) was used according to manufacturer's instructions. DNase treatment (DNA-free™ Kit DNase Treatment & Removal, ambion) was applied to remove remaining DNA. Quality of RNA samples was monitored by Bioanalyzer (Agilent genomics). In brief, RNA was fragmented (150–350 bp) by FastAP buffer (Thermo), end repaired by DNase (Thermo) and FastAP, before sample-specific barcodes were ligated to RNA fragments by T4 RNA ligase 1 (NEB). Samples were purified using the RNA Clean & Concentrator-25 Kit (Zymo); the RiboZero Bacteria Kit (Illumina) was used to remove ribosomal RNA. cDNA libraries were generated using SMARTscribe reverse transcriptase (Clontech). Enrichment was done by AccuPrime HiFi Taq (Thermo) and all purification steps using RNAClean XP beads (Agencourt). Libraries were sequenced in paired-end mode on an Illumina Novaseq 6000 device (2 x 50 bp).

Reads were quality controlled, adapter clipped using fastq-mcf from the ea-utils package [32] and mapped to the reference genome UCBPP-PA14 (NC_008463.1) with bowtie2 [33]. The resulting sam-files were converted to indexed binary format using SAMtools [34]. The program *featureCounts* [35] counted the reads which mapped to genes.

Read counts were used as the basis for further analyses. Differential gene expression analysis of transcriptional profiles of each of the six Tn mutants compared to Tn*ladS* grown under biofilm conditions was performed with the R package edgeR (v.3.20.1) [29]. Normalization factors to scale the raw library sizes were calculated using the weighted trimmed mean of M-values (TMM) method [36]. Reproducibility of biological replicates was analyzed by scatter plots and calculation of the Pearson correlation coefficient of normalized libraries (Supplementary Fig. S3). The obtained p-values for differential expression were adjusted to account for the false-discovery rate using the method by Benjamini and Hochberg [37]. Only genes with an adjusted p-value < 0.05 and an absolute log2FC > 1 were considered differentially expressed.

RNA sequencing of planktonic cultures

Transcriptional profiles of transposon mutants grown under planktonic conditions were recorded as previously described [26]. Briefly, planktonic bacteria were cultivated in 10 ml LB to early stationary phase (OD_{600} of 2) under shaking conditions (37 °C, 180 rpm). Three independent cultures were pooled and an equal volume of RNAprotect (Qiagen) was added prior to cell harvest. RNA was extracted using the RNeasy Mini Kit (Qiagen) and Qiashredder columns (Qiagen) according to the manufacturer's instruction. RNA quality was checked using the RNA Nano Kit on an Agilent Bioanalyzer 2100 (Agilent Technologies). Ribosomal RNA was removed using the Ribo-Zero Bacteria Kit (Illumina) and cDNA libraries were generated with the ScriptSeq v2Kit (Illumina). The samples were sequenced in single-end mode on an Illumina HiSeq 2500 device (1 × 50 bp reads). Mapping was performed using a stampy pipeline [38] with the PA14 genome as a reference. Differential gene expression analysis was performed as described in the previous section.

Results

Abundance of Tn mutants in input and output pools of P. aeruginosa mutant libraries following biofilm growth

We aimed at determining the contribution of non-essential genes of *P. aeruginosa* to overall fitness during conditions of biofilm growth. We therefore generated a Tn mutant library in the two *P. aeruginosa* strains, PA14 and PAO1, as well as in a clinical *P. aeruginosa* respiratory tract isolate (ZG8038581181). To ensure that the near saturated Tn mutant libraries were fully represented in the mutant input pools, we used an inoculum of 2.4×10^6 bacteria and allowed the bacteria to establish biofilms in the wells of a 96-well plate for 48 h.

The biofilm morphologies within a representative well that was inoculated with bacteria of the respective Tn mutant libraries are depicted in Fig. 1 (for replicates see Supplementary Fig. S1). The biofilm phenotypes of all three mutant libraries were recorded by confocal microscopy following 48 h of incubation. Clearly, the three Tn mutant libraries produced distinct biofilm phenotypes. PA14 WT biofilms were loosely connected to the surface and more structured with multi-sized water channels, whereas PAO1 WT produced more dense biofilms with smaller more homogenous water channels. The clinical isolate ZG8038581181 showed an unstructured biofilm phenotype, which has been described previously to be produced repeatedly by a large number of diverse clinical strains [31]. Biofilms of the corresponding Tn mutant libraries showed – despite slight variations in the overall density - very similar structural characteristics that compared well to the corresponding WT strains.

We sequenced two independent input mutant pools of the three Tn mutant libraries (PAO1, PA14 and the clinical isolate). We could confirm a highly saturated homogenous distribution of Tn insertions at the genomic level. To identify genes that influence biofilm growth, we also recovered the Tn mutant library output pools following 48 h of biofilm growth and subjected the recovered bacteria to high-throughput sequencing (three independent output pools). In Table 1 the mean number of Tn disrupted genes that were recovered in the input and output mutant pools of PA14, PAO1 and the clinical isolate is depicted.

Identification of positively and negatively selected Tn mutants during biofilm growth across the three P. aeruginosa strains

Analysis of the output pools from the three *P. aeruginosa* strains following biofilm growth revealed positively and negatively selected Tn mutants. They were ranked according to their false discovery rate (FDR) (Fig. 2). Biofilm growth had a large impact on Tn enrichment (positive selection) and depletion (negative selection). Many Tn mutants were significantly (red dots) enriched during biofilm growth in PA14, PAO1 and ZG8038581181 (112, 255, 128 Tn mutants, respectively) or depleted (45, 49, 263 Tn mutants, respectively).

The overlap of the positively and negatively selected Tn mutants among the three different strains is depicted in Fig. 3. Although the biofilm morphology of all three isolates was quite distinct, we found that a large proportion of genes was negatively (50 genes (14%)) and positively (60 genes (12%)) selected in at least two out of the three *P. aeruginosa* isolates.

Corresponding genes that were affected are listed in Table 2, and enrichment of functional categories of depleted or enriched transposon mutants following biofilm growth are depicted in Fig. 4. From these lists it becomes clear that negative selection in biofilms was mainly observed for genes involved in respiration and oxidative phosphorylation (*nuoF, ccmC, ccmFGH, cc4, cycH, fixG,* PA14_57570), tRNA modification (*gidA, truB, miaA, trmE*), and stress responses (*recB, clpX, ruvB*, *dksA*) indicating that these gene functions are advantageous during growth within a biofilm. We also identified positively selected Tn mutants. Those harbored Tn insertions mainly in genes involved in flagellin biosynthesis and chemotaxis (*fliFGHIJMNOPQR, flhABF, pilCHJU, cheARW*), lactate metabolism (*IldP, IldD*), quorum sensing (*lasR, pqsAB*), and two component systems (*retS, algZ*) suggesting that *P. aeruginosa* strains that have lost these gene functions have a selective advantage under biofilm growth conditions.

Inactivation of genes that were demonstrated to be negatively selected during biofilm growth leads to the production of less robust biofilm structures

We selected overall six genes, which were identified to be negatively selected in at least two out of the three isolate output mutant pools. Three of the genes are encoding tRNA modifying enzymes (*gidA, miaA, truB*), *dksA* encodes a transcriptional regulator that interacts with RNA polymerase and the alarmone ppGpp to alter transcription initiation at target promoters [39], *fixG* encodes a cytochrome c oxidase cbb3 type accessory protein and PA14_57570 a putative cytochrome c reductase. We recorded the growth of the corresponding mutants from the PA14 strain Tn mutant library [19] under planktonic growth conditions (Supplementary Fig. S4) and analyzed their biofilm phenotypes. All tested Tn mutants exhibited slight growth defects and did not reach the same maximum OD_{600} values as the reference stain Tn*ladS* under planktonic conditions. As depicted in Fig. 5 and Supplementary Fig. S2, especially the three mutants with transposon insertions in the genes encoding tRNA modifying enzymes (*gidA, miaA* and *truB*) produced poor biofilms composed of small aggregates, which exhibited overall less biomass (Supplementary Fig. S4). TnPA14_57570 also produced flat biofilms with a reduced biofilm volume and with clusters of dead bacteria, while the Tn*dksA* and Tn*fixG* mutants produced biofilms with structure and biomass comparable to the Tn*ladS* mutant. To rule out that the impaired biofilm phenotypes are due to a general growth defect, we correlated the biofilm volume of the Tn mutants to their maximal optical density during planktonic growth after 24 h (Supplementary Fig. S4D), both relative to Tn*ladS*. Especially for the Tn mutants Tn*miaA*, Tn*truB*, Tn*gidA* and TnPA14_57570, it became clear that the biofilm biomass was lower than would have been expected from their planktonic growth.

To test whether the inactivation of the different genes leads to altered transcriptional responses under biofilm growth conditions, we harvested biofilms of the six Tn mutants after 48 h of growth and recorded the transcriptional profiles as compared to the Tn*ladS* control. Inactivation of the genes encoding the tRNA modifying enzymes *truB, miaA* (but not *gidA*) and *dksA* revealed only a limited amount of significantly differentially expressed genes (34, 11 and 57 genes, respectively) under biofilm conditions. The other three mutants (*fixG,* PA14_57570 and *gidA*) exhibited a higher number of differentially expressed genes (264, 306 and 165 genes, respectively) (see Supplementary Fig. S6 and Supplementary Table S2). Strikingly, we found a common lack of the activation of the alginate biosynthesis gene (*algD*), genes involved in respiration (*nuoA, rnfA*), genes encoding tRNA synthases (tRNA-Ser and tRNA-Leu), and genes involved in the production of cell appendages (*cupB5, pilB, wspA*) in at least three of the six mutants. On the other hand, the transposon mutants seemed to experience enhanced stress, when grown under biofilm conditions. In at least two out of the six mutants we found a relative overexpression of genes encoding for chaperones (*dnaK, dnaJ, clpB*) and heat shock proteins (*hslU, hslV, grpE*), genes involved in flagellar production (*fliC, fliS, flaG*), and antioxidants systems (*trx-1, gpo, lsfA*).

To determine whether the differentially transcribed genes of the Tn mutants are specifically found under biofilm growth conditions, we also recorded the transcriptional profile of three of the six Tn mutants (Tn*miaA*, Tn*gidA*, Tn*dksA*) under planktonic conditions and compared their transcriptional profile to that of the Tn*ladS* control. Under planktonic conditions 37, 316 and 39 genes were differentially regulated in the three respective mutants (Supplementary Table S2). We then compared the genes that were differentially regulated in the three mutants under biofilm conditions to those genes that were regulated under planktonic growth conditions. There was only a minor overlap: 6, 7 and 3 genes, respectively, were differentially expressed in the same direction under both biofilm and planktonic conditions (Supplementary Fig. S5). However, we found in two (Tn*dksa* and Tn*gidA*) out of the three Tn mutants a common lack of activation of the pyochelin biosynthesis (*pchAFGH*), involved in iron assimilation [40] as well as of the heme d1 biosynthesis (*nirEHL*), involved in denitrification under low oxygen conditions [41].

Conclusions

The detection of common responses of bacterial strains to a biofilm growth environment has been a strong focus of previous research. Uncovering core regulatory pathways that drive biofilm formation promises to give clues to novel targets for interfering with biofilm formation.

From previous RNA sequencing and proteomic profiling studies it became clear that important aspects of biofilm formation can be missed [42] and that there is a large inter-strain as well as inter-habitat variation of biofilm-specific gene expression [43,44]. Especially factors that have been previously associated with biofilm growth, such as the production of exopolysaccharides and extracellular cell appendages, are expressed at various times and levels among the different clinical isolates and different biofilm growth conditions [43,45–48]. Nevertheless, it seems that a common theme of biofilm-associated growth is the expression of genes and/or proteins involved in bacterial stress responses [49–54].

While the recording of transcriptional and proteomic responses describes changes in gene expression, genome-wide fitness profiling approaches describe the functional importance of each gene for the expression of a distinct phenotype. Here, to complement previously conducted RNA-seq and proteomic studies, we applied a functional profiling approach and measured the fitness of individual mutants in output versus input mutant pools following biofilm growth. Several previous studies have demonstrated that differentially expressed genes are not necessarily phenotypically important [14,55,56]. Indeed, bacterial genes that change expression upon environmental disturbance are often not among those that matter most in the expression of the respective phenotype [57]. Therefore, transposon sequencing might uncover unexpected functional gene categories that are important for the expression of the biofilm phenotype, and which cannot be detected in transcriptomic and/or proteomic profiling studies.

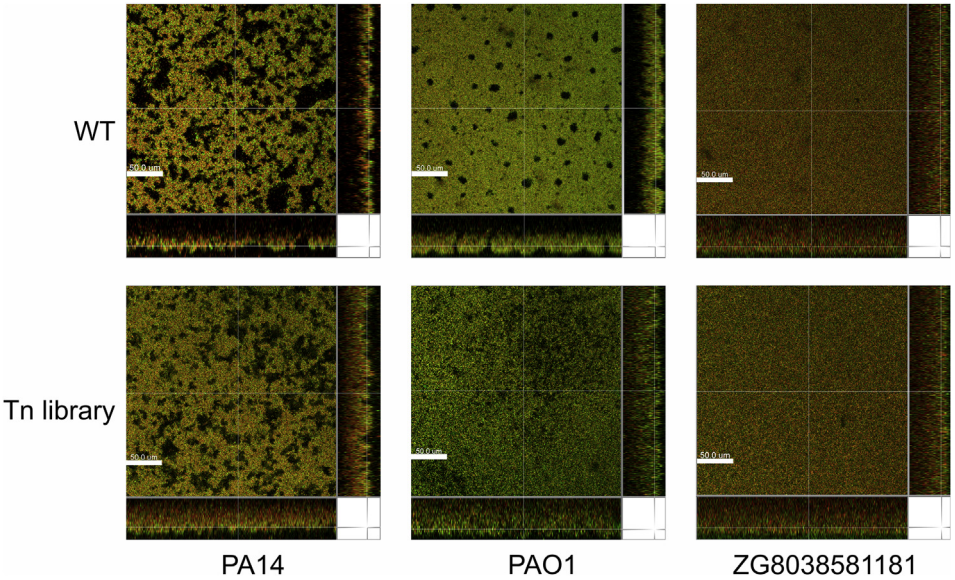

Fig. 1. Biofilm phenotypes of *P. aeruginosa* PA14, PAO1 and a clinical isolate. 96-well plates were inoculated with 2×10^5 bacteria per well of the respective Tn mutant library and biofilms were allowed to establish for 48 h. Images were acquired using confocal laser scanning microscopy (CLSM) following live/dead staining. Living cells are displayed in green (Syto9); dead cells in red (propidium iodide: PI). 3D reconstructions were generated with the Imaris Software. The scale bar represents 50 μm. (For interpretation of the references to colour in this figure legend, the reader is referred to the Web version of this article.)

Table 1
Transposon-disrupted genes in input as well as output mutant pools of strains PA14, PAO1 and ZG8038581181. Only those genes were considered, which were disrupted at least 2 times in the mean of the replicates. SD = standard deviation of replicates.

	PA14	PAO1	ZG8038581181
Number of genes that contain ≥2 TA sites	5826	5537	5965
Number of genes recovered in input mutant pools	4642 (80%) SD (+2%/-4%)	4317 (78%) SD (+3%/-5%)	4952 (83%) SD (+1%/-2%)
Number of genes recovered in output mutant pools	4467 (77%) SD (+4%/-7%)	3659 (66%) SD (+9%/-11%)	4801 (80%) SD (+2%/-2%)

In this study, we show that genes involved in respiration and oxidative phosphorylation are functionally important for biofilm survival. Transposon mutants in *ccmC, ccmFGH, cycH* and *cc4* encoding for components of the cytochrome c1 and c4 complex and in *fixG,* encoding for an accessory cytochrome c oxidase cbb3 type protein, were clearly depleted in output mutant pools during growth within a biofilm. The cytochrome bc_1 and *c*4 complex act as electron donors for the high oxygen affinity reductases, cbb_3-1 and cbb_3-2 [58]. The latter has been demonstrated previously to be induced during growth at low O_2 concentrations [59,60], thus suggesting that adaptation to microaerophilic conditions is an essential biofilm-associated trait. Interestingly, we also found *algZ* mutants to be enriched upon growth within biofilms. AlgZ was demonstrated to be involved in the inhibition of the ccb_3-2 oxidase [61,62], and thus mutations in AlgZ might also lead to higher expression of this high affinity terminal oxidase to promote biofilm growth. Alginate production on the other hand is an important biofilm-associated trait [63]. Interestingly, we found a depletion of *mucD* (negatively affecting *algU* expression [64–66]) mutants and an enrichment of *algU* (positively impacting on alginate production [67])

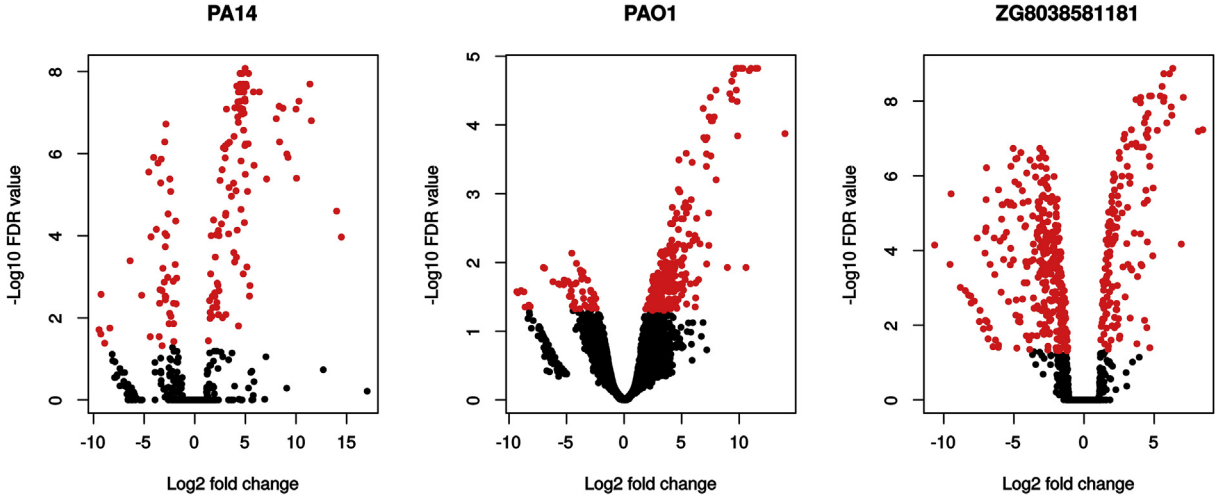

Fig. 2. Positively and negatively enriched Tn mutants in output mutant pools following biofilm growth. Volcano plots show log2 fold enrichment (> 0) or depletion (< 0, x-axis) and false discovery rate (FDR, displayed as log10 value, y-axis) of individual Tn mutants in output mutant pools versus input mutant pools. Red dots indicate Tn mutants with a log2 fold significantly greater than |1|, using the edgeR function glmTREAT and a FDR < 0.05. (For interpretation of the references to colour in this figure legend, the reader is referred to the Web version of this article.)

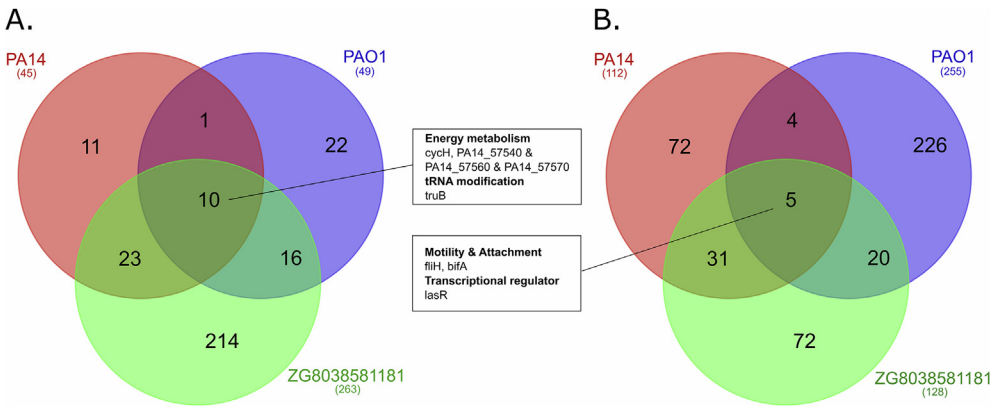

Fig. 3. Venn diagram depicting genes with Tn insertions that were commonly depleted (A) or enriched (B) from output mutant pools in the three strains PA14, PAO1 and a clinical isolate. Only those genes with Tn insertions are listed with a log2 fold change significantly greater than |1| and a FDR < 0.05. Depicted genes correspond to the proportion of genes highlighted in red in Fig. 2. Indicated gene names represent a selection of Tn mutants that were depleted or enriched in the output versus the input pool, respectively. (For interpretation of the references to colour in this figure legend, the reader is referred to the Web version of this article.)

mutants in the output pools. This suggests that, single mutants might benefit from exploiting alginate production by other Tn mutants within the biofilm while they themselves have a growth benefit by avoiding synthesis of this costly polysaccharide.

Apart from the necessity to adapt to microaerophilic conditions, it seems that the switching between aerobic glycolysis and oxidative phosphorylation is essential for biofilm survival as mutants in *lldP* (lactate permease) and *lldD* (lactate dehydrogenase) were positively selected under biofilm growth conditions, whereas mutants in *nuoF* (encoding for a component of the NADH dehydrogenase) and in two enzymes of the TCA cycle, *aceE* (encoding pyruvate dehydrogenase) and *gltA* (encoding citrate synthase) were negatively selected.

Another functional group of genes that was identified to be important for biofilm survival was the SOS-response. In this study, mutants in *recB, clpX and ruvB* were clearly depleted upon growth under biofilm conditions, highlighting the previously described role of a functional SOS response for biofilm formation [68]. In accordance with the finding that the SOS response can be activated by the stringent response [69], we found that mutants of *dksA*, involved in the stringent response [39], are depleted under biofilm growth conditions.

We also identified mutations in several genes involved in tRNA modifications (*gidA, truB, miaA, trmE*) that were depleted from the Tn mutant output pool upon growth under biofilm conditions. There is increasing evidence that tRNA modifications play an important role in the regulation of bacterial pathogenicity traits [70,71]. The decoding properties of tRNAs can be influenced by chemical modifications, which are introduced by tRNA modifying enzymes. Especially when the modification is in the critical anti-codon stem loop, the modification can affect translation efficiency and accuracy and thus modulate the expression of selected genes. As a result, modulation of the tRNA modification activity can influence translation of those genes that exhibit an enrichment of the respective target codons. Clearly, the functional role of tRNA modifications in the growth under biofilm conditions remains to be determined. Of note, a previous study on the essentiality of genes for *P. aeruginosa* adaptation to low oxygen conditions also identified genes involved in tRNA modification (*miaA, truB*) as well as genes involved in DNA repair as being important [17].

To substantiate the role of individual *P. aeruginosa* genes in biofilm formation, we grew six selected mutants under biofilm growth conditions and recorded the transcriptional response. While all mutants were slightly affected in growth under planktonic conditions, the tRNA-modulating enzyme mutants (Tn*miaA,* Tn*truB* and Tn*gidA*) produced biofilms with less biomass, the PA14_57570 mutant produced biofilms with clusters of dead bacteria, while Tn*fixG* and the stringent response mutant (Tn*dksA*) produced biofilms that were similar to the reference strain Tn*ladS*. Of note, transcriptional profiling of the biofilm grown mutant strains revealed that they seemed to experience stress as opposed to *P. aeruginosa* wild type biofilm grown cells. We found the upregulation of several stress-responses as a common theme only under biofilm but not under planktonic growth conditions. These responses included higher expression of heat shock proteins, chaperones, and universal stress proteins in the selected mutants. Thus, although the disturbance of *P. aeruginosa* biofilm growth was achieved by the introduction of a very diverse array of mutations (affecting respiration, tRNA modification or the stringent response), we found the induction of very similar stress response genes if grown under biofilm conditions. This indicates that there may be a common biofilm-specific way to induce a survival program that could also become an interesting target for the development of novel anti-biofilm therapeutic strategies.

A well-known outcome of chronic *P. aeruginosa* infections in the CF lung is the selection for LasR mutations and it was hypothesized that a *lasR* mutant might favor the shift to a more immunogenic phenotype, as the anti-flagellin proteolytic activities of the LasR-governed LasB and AprA are decreased [72]. However, the results of our Tn-seq experiment, implies that loss of *lasR* also confers a selective advantage under in vitro biofilm-associated growth conditions. Interestingly, not only *lasR* mutants but also *rpoS* mutants were enriched under biofilm conditions. LasR and RpoS are known to interact and to co-regulate many genes [73–75]. Furthermore, mutants in *retS*, encoding for a sensor kinase, have recently been directly demonstrated to produce more biofilms and to exhibit high levels of c-di-GMP [76]. Mutants of *retS* and *rsmA* were demonstrated to show similar phenotypes with overproduction of exopolysaccharides, reduced expression of T3SS, and diminished type IV pili motility [77,78]. In accordance, mutants in both genes were clearly enriched upon biofilm growth in this study.

Finally, a number of mutants, which were affected in chemotaxis and bacterial motility as well as in genes of the alkyl-quinolone signaling system (*pqsA, pqsB*) were positively selected under biofilm conditions. This indicates that loss of motility as well as PQS production positively impacts bacterial survival under biofilm conditions. However, it is conceivable that these Tn mutants are only positively selected when e.g. signaling molecule negative mutants do not exceed a certain threshold level in the biofilm population.

In conclusion, in this study we have identified both known and novel genetic determinants of biofilm survival. Results from previous publications already suggested a role of alginate production, adaptation to microaerophilic conditions, metabolic switching, induction of an SOS and stringent response as well as reduced expression of the LasR quorum sensing system, and downregulation of motility, in biofilm formation. However, our results also highlight the success of our transposon sequencing approach in the identification of intriguing new players involved in biofilm survival. Elucidating e.g. the role of tRNA modifications in biofilm survival will be an exciting future challenge.

Table 2
Significantly depleted (A) or enriched (B) genes with Tn insertions in output mutant pools of PA14, PAO1 and the clinical isolate ZG8038581181 following biofilm growth. A total of 110 Tn mutants exhibited an enrichment or depletion in output versus input mutant pools in at least two out of three strains. Log2-fold change values [log2FC] in bold indicate a depletion/enrichment (FDR $\leq$ 0.05) significantly greater than log2FC of |1|. Log2FC values are conditionally highlighted relative within a condition ranging from red (low value) over yellow (intermediate) to green (high value).

A.	negatively selected Tn mutants						
		PA14		PAO1		ZG8038581181	
	PA14 locus	log2FC	FDR	log2FC	FDR	log2FC	FDR
PA14+ PAO1+ ZG8038581181	PA14_14910	**-2,77**	9,94E-05	**-5,21**	1,80E-02	**-3,85**	3,82E-07
	PA14_45280,cycH	**-2,09**	4,43E-03	**-4,17**	1,99E-02	**-4,35**	5,30E-06
	PA14_45350,ccmC	**-8,39**	1,78E-02	**-4,87**	1,88E-02	**-5,72**	4,39E-05
	PA14_57540	**-2,54**	1,39E-02	**-4,24**	4,74E-02	**-5,21**	5,28E-06
	PA14_57560	**-2,38**	8,34E-06	**-3,81**	1,29E-02	**-4,87**	3,55E-07
	PA14_57570	**-2,48**	7,79E-03	**-3,57**	1,37E-02	**-4,53**	1,40E-05
	PA14_57870	**-3,63**	1,70E-06	**-3,85**	4,71E-02	**-1,54**	1,40E-02
	PA14_62730,truB	**-1,88**	4,38E-05	**-6,18**	1,91E-02	**-3,18**	3,36E-07
	PA14_68670	**-9,45**	1,94E-02	**-4,14**	1,03E-02	**-6,96**	6,11E-07
	PA14_70560	**-4,06**	1,24E-06	**-6,92**	1,21E-02	**-3,27**	4,98E-06
PAO1+ ZG8038581181	PA14_09530,mexH	-0,24	1,00E+00	**-2,88**	2,66E-02	**-2,41**	2,13E-04
	PA14_11720	-0,07	1,00E+00	**-3,12**	4,46E-02	**-2,28**	3,62E-06
	PA14_17930,glpD	-1,33	5,18E-01	**-2,83**	4,64E-02	**-3,09**	1,52E-06
	PA14_29970,nuoF	-1,21	9,66E-01	**-2,71**	3,79E-02	**-3,02**	6,03E-05
	PA14_38490,gnyL	-1,51	1,00E+00	**-3,52**	3,34E-02	**-3,13**	8,22E-05
	PA14_38530,fahA	-0,27	1,00E+00	**-5,24**	2,11E-02	**-2,89**	2,57E-05
	PA14_41230,clpX	-0,75	1,00E+00	**-3,68**	1,75E-02	**-3,16**	5,08E-06
	PA14_44070,gltA	-3,36	9,60E-02	**-7,01**	1,18E-02	**-2,79**	1,16E-03
	PA14_45290,ccmH	-7,39	4,55E-01	**-4,60**	2,11E-02	**-6,70**	2,36E-04
	PA14_45300,ccmG	-7,01	3,52E-01	**-4,60**	2,59E-02	**-8,46**	1,19E-03
	PA14_45310,ccmF	-7,88	1,18E-01	**-5,59**	2,10E-02	**-7,06**	1,18E-04
	PA14_45640,fleN	1,51	4,55E-01	**-3,52**	1,66E-02	**-4,93**	1,45E-06
	PA14_55670,recB	-3,92	2,11E-01	**-4,38**	4,19E-02	**-10,65**	7,16E-05
	PA14_62490,dksA	-1,64	6,48E-01	**-8,16**	4,37E-02	**-3,17**	1,96E-04
	PA14_67720,secB	-1,50	4,93E-01	**-9,23**	2,75E-02	**-2,92**	1,84E-05
	PA14_72460,cc4	-1,30	1,00E+00	**-4,54**	7,33E-03	**-3,32**	3,16E-05
PA14+ PAO1	PA14_44430	**-3,43**	2,06E-03	**-3,71**	1,46E-02	-	-
PA14+ ZG8038581181	PA14_00120	**-2,13**	1,28E-03	-2,13	7,56E-02	**-1,50**	8,47E-03
	PA14_03880,spuB	**-3,31**	1,36E-06	-2,12	1,38E-01	**-5,05**	1,86E-07
	PA14_05520,mexR	**-2,64**	2,94E-05	-3,87	5,25E-02	**-2,17**	2,12E-03
	PA14_22910,edd	**-2,90**	3,64E-03	0,74	7,68E-01	**-5,98**	5,58E-05
	PA14_23280,pheA	**-9,26**	2,68E-03	0,10	1,00E+00	**-8,08**	1,67E-03
	PA14_25390,sth	**-3,23**	4,79E-02	1,85	3,21E-01	**-2,76**	1,14E-04
	PA14_41570,oprF	**-3,24**	2,17E-03	-2,21	1,79E-01	**-3,25**	6,72E-06
	PA14_44420,fixG	**-1,93**	5,02E-04	-0,64	7,81E-01	**-1,76**	3,83E-04
	PA14_49170,phoQ	**-6,39**	4,07E-04	-2,55	1,98E-01	**-5,47**	5,06E-06
	PA14_51780,ruvB	**-3,47**	4,43E-03	-1,41	4,15E-01	**-5,26**	2,44E-04
	PA14_54390,mucD	**-3,15**	6,19E-04	0,87	6,55E-01	**-4,50**	2,40E-07
	PA14_58930	**-9,28**	2,49E-02	-0,60	8,01E-01	**-3,66**	1,19E-05
	PA14_62900,greA	**-3,51**	2,88E-02	-3,35	7,35E-02	**-3,52**	1,08E-04
	PA14_65320,miaA	**-2,92**	2,95E-03	-8,24	5,31E-02	**-4,79**	4,11E-02
	PA14_65410,orn	**-4,40**	2,88E-02	-8,06	9,08E-02	**-3,06**	1,84E-04
	PA14_65750,ompH	**-1,79**	1,07E-03	-0,35	8,95E-01	**-1,92**	5,24E-05
	PA14_66290,aceE	**-5,25**	2,82E-03	-	-	**-6,40**	4,64E-05
	PA14_66980,tatC	**-2,07**	3,76E-02	-4,44	5,04E-02	**-5,53**	3,28E-05
	PA14_69070,yhiH	**-2,85**	1,90E-07	-0,24	9,25E-01	**-1,31**	6,62E-03
	PA14_71640	**-2,09**	1,39E-02	-3,17	5,71E-02	**-4,09**	8,48E-07
	PA14_73370,gidA	**-4,54**	2,80E-06	-3,77	5,23E-02	**-7,02**	3,09E-05
	PA14_73400,trmE	**-4,32**	1,06E-04	-1,77	2,46E-01	**-9,55**	2,36E-04

B.	positively selected Tn mutants						
		PA14		PAO1		ZG8038581181	
		log2FC	FDR	log2FC	FDR	log2FC	FDR
PA14+ PAO1+ ZG8038581181	PA14_28130	**11,52**	1,58E-07	**4,17**	1,43E-02	**6,33**	1,33E-09
	PA14_45960,lasR	**4,35**	7,82E-08	**4,35**	2,04E-02	**3,05**	1,69E-07
	PA14_49880	**14,01**	2,51E-05	**5,43**	4,02E-02	**4,29**	5,49E-06
	PA14_50110,fliH	**5,31**	1,11E-08	**2,42**	3,96E-02	**3,33**	3,03E-04
	PA14_56790	**4,73**	1,07E-07	**3,97**	1,04E-02	**4,02**	1,12E-08
PAO1+ ZG8038581181	PA14_02730	-0,06	1,00E+00	**6,47**	1,78E-02	**1,59**	1,19E-02
	PA14_04410,ptsP	-0,47	1,00E+00	**5,40**	2,59E-04	**5,56**	4,08E-09
	PA14_17470,nlpD	1,14	1,00E+00	**5,07**	2,10E-02	**5,69**	1,86E-09
	PA14_17480,rpoS	1,14	1,00E+00	**7,34**	1,91E-03	**8,46**	5,87E-08
	PA14_20290,algZ	1,49	1,44E-01	**2,68**	4,48E-02	**4,03**	3,59E-05
	PA14_20800	0,51	1,00E+00	**5,63**	3,86E-03	**1,82**	1,28E-03
	PA14_22490,acpD	0,37	1,00E+00	**5,02**	2,11E-02	**1,69**	7,40E-04
	PA14_33960	0,09	1,00E+00	**3,90**	2,68E-02	**2,72**	9,89E-06
	PA14_41670,ppsA	0,64	1,00E+00	**3,42**	4,46E-02	**1,69**	6,87E-05
	PA14_41900,panE	0,75	1,00E+00	**4,02**	7,01E-03	**4,68**	7,35E-09
	PA14_51340,mvfR	0,49	1,00E+00	**4,76**	3,22E-04	**8,15**	6,46E-08
	PA14_51420,pqsB	0,11	1,00E+00	**2,35**	2,55E-02	**5,67**	1,03E-08
	PA14_51430,pqsA	0,16	1,00E+00	**5,16**	2,52E-02	**6,22**	1,44E-08
	PA14_52570,rsmA	7,03	8,88E-02	**7,15**	4,01E-04	**2,33**	3,84E-03
	PA14_53140	-0,12	1,00E+00	**2,81**	3,43E-02	**4,04**	7,98E-09
	PA14_58760,pilC	1,42	1,00E+00	**10,25**	1,50E-05	**4,40**	2,78E-08
	PA14_60280,fimU	-0,40	1,00E+00	**11,03**	1,50E-05	**1,77**	3,34E-05
	PA14_62710,pnp	-0,41	1,00E+00	**4,28**	4,17E-02	**4,31**	7,39E-03
	PA14_64230,retS	5,54	2,14E-01	**6,93**	1,53E-04	**2,06**	2,18E-05
	PA14_72450,dsbA	3,93	4,62E-01	**2,62**	3,78E-02	**3,28**	1,05E-06
PA14 + PAO1	PA14_30040	**2,34**	8,45E-03	**2,53**	2,77E-02	-	-
	PA14_40030	**2,17**	5,60E-03	**2,91**	1,78E-02	-	-
	PA14_05190,pilU	**2,83**	7,20E-07	**7,08**	1,64E-04	0,45	1,00E+00
	PA14_53310	**8,34**	7,01E-08	**3,59**	7,58E-03	-0,66	1,00E+00
PA14+ ZG8038581181	PA14_03720	**3,42**	5,29E-07	-0,75	7,41E-01	**2,51**	1,25E-04
	PA14_20760,cheR	**2,49**	4,50E-06	-1,52	5,06E-01	**2,06**	3,49E-06
	PA14_40600	**11,37**	2,02E-08	7,18	1,87E-01	**6,94**	2,55E-05
	PA14_40620	**3,86**	2,57E-04	4,04	1,58E-01	**3,70**	5,59E-07
	PA14_44300,aer	**6,38**	3,14E-08	0,68	7,71E-01	**3,78**	5,68E-06
	PA14_45500,cheW	**3,25**	5,71E-07	-1,26	4,04E-01	**2,46**	2,38E-07
	PA14_45590,cheA	**2,99**	7,58E-07	-2,61	1,21E-01	**3,08**	1,35E-07
	PA14_45660,flhF	**3,96**	7,62E-08	1,85	1,57E-01	**4,41**	2,46E-06
	PA14_45680,flhA	**5,10**	2,32E-08	1,32	3,35E-01	**4,30**	6,67E-03
	PA14_45720,flhB	**4,86**	1,03E-07	1,88	1,24E-01	**2,23**	9,44E-08
	PA14_45740,fliR	**4,99**	3,19E-06	1,71	1,23E-01	**4,52**	8,96E-06
	PA14_45760,fliQ	**4,66**	3,14E-08	0,38	9,25E-01	**3,13**	2,36E-04
	PA14_45770,fliP	**5,85**	1,93E-06	1,51	2,03E-01	**4,93**	2,16E-08
	PA14_45780,fliO	**5,41**	2,95E-03	1,32	3,54E-01	**4,48**	5,37E-04
	PA14_45790,fliN	**4,98**	8,34E-09	1,68	1,57E-01	**4,12**	1,35E-06
	PA14_45800,fliM	**4,71**	1,11E-08	1,17	4,87E-01	**4,56**	7,78E-08
	PA14_45830	**4,48**	2,02E-08	1,21	4,30E-01	**1,44**	4,07E-05
	PA14_50080,fliJ	**4,76**	2,85E-08	1,11	4,58E-01	**1,59**	7,35E-09
	PA14_50100,fliI	**4,85**	3,14E-08	2,06	8,55E-02	**2,90**	2,56E-04
	PA14_50130,fliG	**5,02**	5,81E-07	1,43	2,46E-01	**4,52**	2,47E-03
	PA14_50140,fliF	**4,94**	4,63E-08	1,25	3,61E-01	**4,80**	5,93E-05
	PA14_50180,fleR	**4,98**	5,27E-08	1,04	5,14E-01	**1,35**	4,53E-06
	PA14_50200,fleS	**4,60**	2,75E-08	0,90	6,39E-01	**2,19**	3,86E-08
	PA14_50220,fleQ	**4,57**	1,51E-06	0,86	6,66E-01	**4,53**	1,16E-02
	PA14_53300	**8,38**	5,19E-07	0,21	9,58E-01	**2,21**	1,71E-07
	PA14_54430,algU	**1,52**	7,37E-03	2,22	3,62E-01	**1,68**	2,13E-06
	PA14_63080,lldP	**8,71**	7,82E-08	-0,05	9,84E-01	**5,70**	1,65E-07
	PA14_63090,lldD	**5,79**	3,14E-08	0,24	9,42E-01	**4,06**	4,82E-05
	PA14_65200,rnr	**4,79**	8,50E-04	1,15	4,95E-01	**2,08**	7,98E-09
	PA14_66320	**10,00**	8,22E-08	0,80	7,10E-01	**6,09**	1,86E-09
	PA14_66330,msrA	**2,40**	9,94E-05	2,44	5,13E-01	**1,99**	6,77E-05

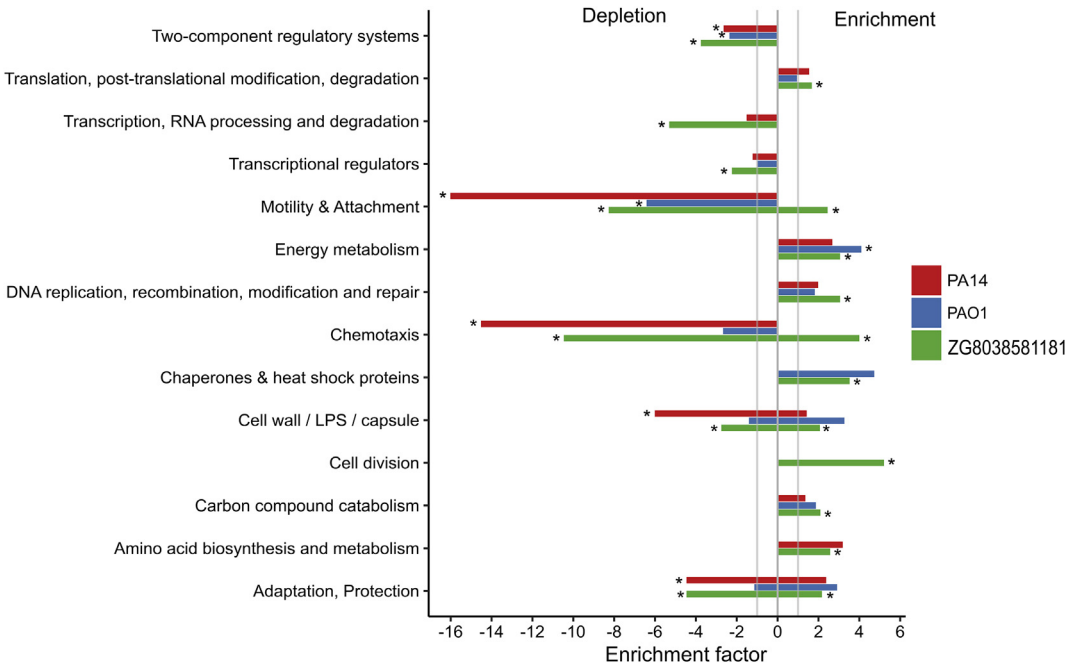

Fig. 4. Functional enrichment of genes with Tn insertions during biofilm growth. Genes with Tn insertions of the three *P. aeruginosa* Tn mutant libraries (PA14, PAO1, clinical isolate ZG8038581181), which were enriched/depleted in output mutant as compared to input mutant pools following biofilm growth were assigned to PseudoCAP categories. The left panel shows the enrichment of functional categories for all Tn mutants depleted under biofilm conditions (decreased fitness) and the right panel shows the functional enrichment for those Tn mutants which are enriched in biofilms (increased fitness). The enrichment factor indicates the proportion of genes within a certain function (PseudoCAP) relative to the gene proportion expected by chance. Asterisks indicate parameters that show statistically significantly enriched functions (FDR < 0.05) as determined by hypergeometrical distribution.

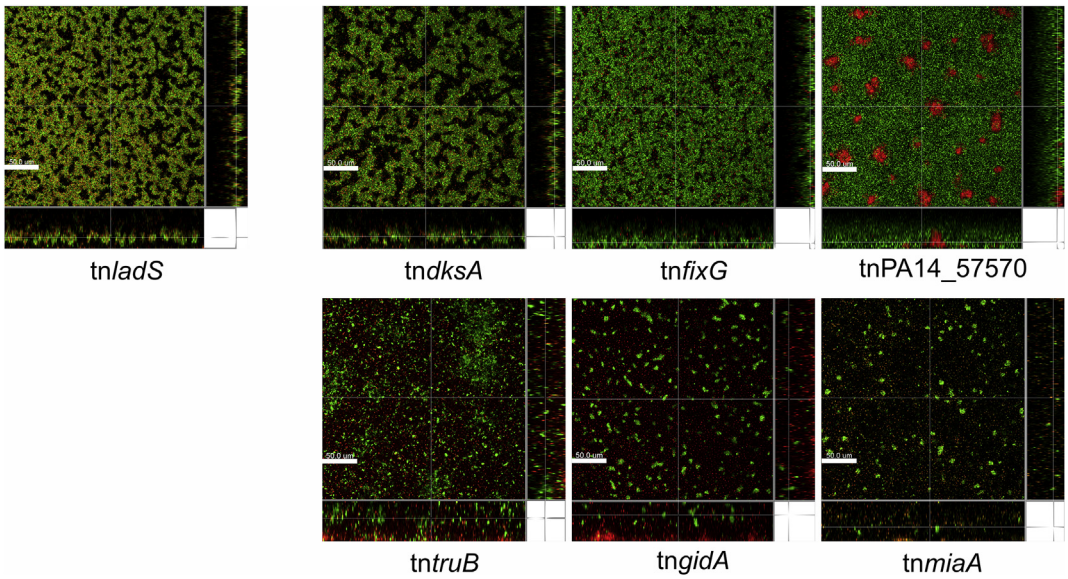

Fig. 5. Biofilm phenotypes of six selected Tn mutants as compared to the wild-type control (Tn*ladS*). Biofilms were grown for 48 h in a microtiter plate-based in vitro biofilm assay; images were acquired using confocal laser scanning microscopy (CLSM) following live/dead staining. Living cells are displayed in green (Syto9); dead cells in red (propidium iodide: PI). 3D reconstructions were generated with the Imaris Software. The scale bar represents 50 μm. (For interpretation of the references to colour in this figure legend, the reader is referred to the Web version of this article.)

Acknowledgements

S.H. was funded by the EU (ERC Consolidator Grant COMBAT 724290) and received funding from the Deutsche Forschungsgemeinschaft (DFG, German Research Foundation) in the DFG SPP 1879 program and under Germany's Excellence Strategy – EXC 2155 "RESIST" – Project ID 39087428. We thank Ethna Fidelma Boyd (University of Delaware) for providing *E. coli* β2155 λpir [79], Michal Koska for recording growth curves, and Astrid Dröge, Agnes Nielsen and Anja Kobold (Helmholtz Centre for Infection Research) for technical assistance.

Appendix A. Supplementary data

Supplementary data to this article can be found online at https://doi.org/10.1016/j.biofilm.2020.100023.

References

[1] Fong JNC, Yildiz FH. Biofilm matrix proteins. Microbiol Spectr 2015;3(2).
[2] Hall CW, Mah TF. Molecular mechanisms of biofilm-based antibiotic resistance and tolerance in pathogenic bacteria. FEMS Microbiol Rev 2017;41(3):276–301.
[3] Limoli DH, Jones CJ, Wozniak DJ. Bacterial extracellular polysaccharides in biofilm formation and function. Microbiol Spectr 2015;3(3).
[4] Hall-Stoodley L, Stoodley P. Biofilm formation and dispersal and the transmission of human pathogens. Trends Microbiol 2005;13(1):7–10.
[5] Hoiby N, Ciofu O, Johansen HK, Song ZJ, Moser C, Jensen PO, Molin S, Givskov M, Tolker-Nielsen T, Bjarnsholt T. The clinical impact of bacterial biofilms. Int J Oral Sci 2011;3(2):55–65.
[6] Römling U, Balsalobre C. Biofilm infections, their resilience to therapy and innovative treatment strategies. J Intern Med 2012;272(6):541–61.
[7] Moradali MF, Ghods S, Rehm BH. *Pseudomonas aeruginosa* lifestyle: a paradigm for adaptation, survival, and persistence. Front Cell Infect Microbiol 2017;7:39.
[8] Barquist L, Mayho M, Cummins C, Cain AK, Boinett CJ, Page AJ, Langridge GC, Quail MA, Keane JA, Parkhill J. The TraDIS toolkit: sequencing and analysis for dense transposon mutant libraries. Bioinformatics 2016;32(7):1109–11.
[9] Langridge GC, Phan MD, Turner DJ, Perkins TT, Parts L, Haase J, Charles I, Maskell DJ, Peters SE, Dougan G, et al. Simultaneous assay of every *Salmonella Typhi* gene using one million transposon mutants. Genome Res 2009;19(12):2308–16.
[10] Barquist L, Boinett CJ, Cain AK. Approaches to querying bacterial genomes with transposon-insertion sequencing. RNA Biol 2013;10(7):1161–9.
[11] Cameron DR, Shan Y, Zalis EA, Isabella V, Lewis K. A genetic determinant of persister cell formation in bacterial pathogens. J Bacteriol 2018;200(17).
[12] Gallagher LA, Shendure J, Manoil C. Genome-scale identification of resistance functions in *Pseudomonas aeruginosa* using Tn-seq. MBio 2011;2(1). e00315-00310.
[13] Lorenz A, Preusse M, Bruchmann S, Pawar V, Grahl N, Pils MC, Nolan LM, Filloux A, Weiss S, Häussler S. Importance of flagella in acute and chronic *Pseudomonas aeruginosa* infections. Environ Microbiol 2019;21(3):883–97.
[14] Turner KH, Everett J, Trivedi U, Rumbaugh KP, Whiteley M. Requirements for *Pseudomonas aeruginosa* acute burn and chronic surgical wound infection. PLoS Genet 2014;10(7):e1004518.
[15] Nolan LM, Whitchurch CB, Barquist L, Katrib M, Boinett CJ, Mayho M, Goulding D, Charles IG, Filloux A, Parkhill J, et al. A global genomic approach uncovers novel components for twitching motility-mediated biofilm expansion in *Pseudomonas aeruginosa*. Microb Genom 2018;4(11).
[16] Lee SA, Gallagher LA, Thongdee M, Staudinger BJ, Lippman S, Singh PK, Manoil C. General and condition-specific essential functions of *Pseudomonas aeruginosa*. Proc Natl Acad Sci U S A 2015;112(16):5189–94.
[17] Basta DW, Bergkessel M, Newman DK. Identification of fitness determinants during energy-limited growth arrest in *Pseudomonas aeruginosa*. MBio 2017;8(6).
[18] Chao MC, Abel S, Davis BM, Waldor MK. The design and analysis of transposon insertion sequencing experiments. Nat Rev Microbiol 2016;14:119–28.
[19] Liberati NT, Urbach JM, Miyata S, Lee DG, Drenkard E, Wu G, Villanueva J, Wei T, Ausubel FM. An ordered, nonredundant library of *Pseudomonas aeruginosa* strain PA14 transposon insertion mutants. In: Proceedings of the national academy of sciences, vol. 103; 2006. p. 2833–8.
[20] Kulasekara HD. Transposon mutagenesis. Methods Mol Biol 2014;1149:501–19.
[21] Müsken M, Di Fiore S, Römling U, Häussler S. A 96-well-plate–based optical method for the quantitative and qualitative evaluation of *Pseudomonas aeruginosa* biofilm formation and its application to susceptibility testing. In: Nature protocols, vol. 5; 2010. p. 1460–9.
[22] Nocker A, Cheung C-Y, Camper AK. Comparison of propidium monoazide with ethidium monoazide for differentiation of live vs. dead bacteria by selective removal of DNA from dead cells. 2006.
[23] Tavernier S, Coenye T. Quantification of *Pseudomonas aeruginosa* in multispecies biofilms using PMA-qPCR. PeerJ 2015;3:e787.
[24] Martin M. Cutadapt removes adapter sequences from high-throughput sequencing reads. EMBnetjournal 2011;17:10.
[25] Bankevich A, Nurk S, Antipov D, Gurevich AA, Dvorkin M, Kulikov AS, Lesin VM, Nikolenko SI, Pham S, Prjibelski AD, et al. SPAdes: a new genome assembly algorithm and its applications to single-cell sequencing. J Comput Biol 2012;19(5):455–77.
[26] Khaledi A, Weimann A, Schniederjans M, Asgari E, Kuo T-H, Oliver A, Cabot G, Kola A, Gastmeier P, Hogardt M, et al. Fighting antimicrobial resistance in *Pseudomonas aeruginosa* with machine learning-enabled molecular diagnostics. bioRxiv 2019:643676.
[27] Seemann T. Prokka: rapid prokaryotic genome annotation. Bioinformatics 2014;30(14):2068–9.
[28] Team RCR. A language and environment for statistical computing. Vienna, Austria: R Foundation for Statistical Computing; 2019.
[29] Robinson MD, McCarthy DJ, Smyth GK. edgeR: a Bioconductor package for differential expression analysis of digital gene expression data. Bioinformatics 2010;26(1):139–40.
[30] Heberle H, Meirelles GV, da Silva FR, Telles GP, Minghim R. InteractiVenn: a web-based tool for the analysis of sets through Venn diagrams. BMC Bioinf 2015;16:169.
[31] Thöming JG, Tomasch J, Preusse M, Koska M, Grahl N, Pohl S, Willger SD, Kaever V, Müsken M, Häussler S. Parallel evolutionary paths to produce more than one *Pseudomonas aeruginosa* biofilm phenotype. NPJ Biofilms Microbiomes 2020;6:2.
[32] Aronesty E. Comparison of sequencing utility programs. Open Bioinf J 2013;7:1–8.
[33] Langmead B, Salzberg SL. Fast gapped-read alignment with Bowtie 2. Nat Methods 2012;9(4):357–9.
[34] Li H, Handsaker B, Wysoker A, Fennell T, Ruan J, Homer N, Marth G, Abecasis G, Durbin R. Genome project data processing S: the sequence alignment/map format and SAMtools. Bioinformatics 2009;25(16):2078–9.
[35] Liao Y, Smyth GK, Shi W. featureCounts: an efficient general purpose program for assigning sequence reads to genomic features. Bioinformatics 2014;30(7):923–30.
[36] Robinson MD, Oshlack A. A scaling normalization method for differential expression analysis of RNA-seq data. Genome Biol 2010;11(3):R25.
[37] Benjamini Y, Hochberg Y. Controlling the false discovery rate: a practical and powerful approach to multiple testing. In: Journal of the royal statistical society series B (methodological), vol. 57. WileyRoyal Statistical Society; 1995. p. 289–300.
[38] Lunter G, Goodson M. Stampy: a statistical algorithm for sensitive and fast mapping of Illumina sequence reads. Genome Res 2011;21(6):936–9.
[39] Ross W, Sanchez-Vazquez P, Chen AY, Lee JH, Burgos HL, Gourse RL. ppGpp binding to a site at the RNAP-DksA interface accounts for its dramatic effects on transcription initiation during the stringent response. Mol Cell 2016;62(6):811–23.
[40] Braud A, Hannauer M, Mislin GL, Schalk IJ. The *Pseudomonas aeruginosa* pyochelin-iron uptake pathway and its metal specificity. J Bacteriol 2009;191(11):3517–25.
[41] Storbeck S, Walther J, Muller J, Parmar V, Schiebel HM, Kemken D, Dulcks T, Warren MJ, Layer G. The *Pseudomonas aeruginosa* nirE gene encodes the S-adenosyl-L-methionine-dependent uroporphyrinogen III methyltransferase required for heme d(1) biosynthesis. FEBS J 2009;276(20):5973–82.
[42] An D, Parsek MR. The promise and peril of transcriptional profiling in biofilm communities. Curr Opin Microbiol 2007;10(3):292–6.
[43] Erdmann J, Thöming JG, Pohl S, Pich A, Lenz C, Häussler S. The core proteome of biofilm-grown clinical *Pseudomonas aeruginosa* isolates. Cells 2019;8(10).
[44] Patell S, Gu M, Davenport P, Givskov M, Waite RD, Welch M. Comparative microarray analysis reveals that the core biofilm-associated transcriptome of *Pseudomonas aeruginosa* comprises relatively few genes. Environ Microbiol Rep 2010;2(3):440–8.
[45] Southey-Pillig CJ, Davies DG, Sauer K. Characterization of temporal protein production in *Pseudomonas aeruginosa* biofilms. J Bacteriol 2005;187(23):8114–26.
[46] Sauer K. The genomics and proteomics of biofilm formation. Genome Biol 2003;4(6):219.
[47] Sauer K, Camper AK, Ehrlich GD, Costerton JW, Davies DG. *Pseudomonas aeruginosa* displays multiple phenotypes during development as a biofilm. J Bacteriol 2002;184(4):1140–54.
[48] Tolker-Nielsen T. Biofilm development. Microbiol Spectr 2015;3(2). MB-0001-2014.
[49] Wood TK. Insights on *Escherichia coli* biofilm formation and inhibition from whole-transcriptome profiling. Environ Microbiol 2009;11(1):1–15.
[50] Bayramoglu B, Toubiana D, Gillor O. Genome-wide transcription profiling of aerobic and anaerobic *Escherichia coli* biofilm and planktonic cultures. FEMS Microbiol Lett 2017;364(3).
[51] Domka J, Lee J, Bansal T, Wood TK. Temporal gene-expression in *Escherichia coli* K-12 biofilms. Environ Microbiol 2007;9(2):332–46.
[52] Beloin C, Valle J, Latour-Lambert P, Faure P, Kzreminski M, Balestrino D, Haagensen JA, Molin S, Prensier G, Arbeille B, et al. Global impact of mature biofilm lifestyle on *Escherichia coli* K-12 gene expression. Mol Microbiol 2004;51(3):659–74.
[53] Schembri MA, Kjaergaard K, Klemm P. Global gene expression in *Escherichia coli* biofilms. Mol Microbiol 2003;48(1):253–67.
[54] Stewart PS, Franklin MJ, Williamson KS, Folsom JP, Boegli L, James GA. Contribution of stress responses to antibiotic tolerance in *Pseudomonas aeruginosa* biofilms. Antimicrob Agents Chemother 2015;59(7):3838–47.
[55] Smith JJ, Sydorskyy Y, Marelli M, Hwang D, Bolouri H, Rachubinski RA, Aitchison JD. Expression and functional profiling reveal distinct gene classes involved in fatty acid metabolism. Mol Syst Biol 2006;2:2006. 0009.
[56] Bielecki P, Komor U, Bielecka A, Müsken M, Puchałka J, Pletz MW, Ballmann M, Martins dos Santos VA, Weiss S, Häussler S. *Ex vivo* transcriptional profiling reveals a common set of genes important for the adaptation of *Pseudomonas aeruginosa* to chronically infected host sites. Environ Microbiol 2013;15:570–87.
[57] Jensen PA, Zhu Z, van Opijnen T. Antibiotics disrupt coordination between transcriptional and phenotypic stress responses in pathogenic bacteria. Cell Rep 2017;20(7):1705–16.
[58] Jo J, Price-Whelan A, Dietrich LE. An aerobic exercise: defining the roles of *Pseudomonas aeruginosa* terminal oxidases. J Bacteriol 2014;196(24):4203–5.
[59] Comolli JC, Donohue TJ. Differences in two *Pseudomonas aeruginosa* cbb3 cytochrome oxidases. Mol Microbiol 2004;51(4):1193–203.
[60] Kawakami T, Kuroki M, Ishii M, Igarashi Y, Arai H. Differential expression of multiple terminal oxidases for aerobic respiration in *Pseudomonas aeruginosa*. Environ Microbiol 2010;12(6):1399–412.
[61] Lizewski SE, Schurr JR, Jackson DW, Frisk A, Carterson AJ, Schurr MJ. Identification of AlgR-regulated genes in *Pseudomonas aeruginosa* by use of microarray analysis. J Bacteriol 2004;186(17):5672–84.
[62] Okkotsu Y, Little AS, Schurr MJ. The *Pseudomonas aeruginosa* AlgZR two-component system coordinates multiple phenotypes. Front Cell Infect Microbiol 2014;4:82.
[63] Bazire A, Shioya K, Soum-Soutera E, Bouffartigues E, Ryder C, Guentas-Dombrowsky L, Hemery G, Linossier I, Chevalier S, Wozniak DJ, et al. The sigma factor AlgU plays a key role in formation of robust biofilms by nonmucoid *Pseudomonas aeruginosa*. J Bacteriol 2010;192(12):3001–10.
[64] Boucher JC, Martinez-Salazar J, Schurr MJ, Mudd MH, Yu H, Deretic V. Two distinct loci affecting conversion to mucoidy in *Pseudomonas aeruginosa* in cystic fibrosis encode homologs of the serine protease HtrA. J Bacteriol 1996;178(2):511–23.

[65] Wood LF, Ohman DE. Independent regulation of MucD, an HtrA-like protease in *Pseudomonas aeruginosa*, and the role of its proteolytic motif in alginate gene regulation. J Bacteriol 2006;188(8):3134–7.
[66] Yorgey P, Rahme LG, Tan MW, Ausubel FM. The roles of mucD and alginate in the virulence of *Pseudomonas aeruginosa* in plants, nematodes and mice. Mol Microbiol 2001;41(5):1063–76.
[67] Govan JR, Deretic V. Microbial pathogenesis in cystic fibrosis: mucoid *Pseudomonas aeruginosa* and Burkholderia cepacia. Microbiol Rev 1996;60(3):539–74.
[68] Chellappa ST, Maredia R, Phipps K, Haskins WE, Weitao T. Motility of *Pseudomonas aeruginosa* contributes to SOS-inducible biofilm formation. Res Microbiol 2013; 164(10):1019–27.
[69] Strugeon E, Tilloy V, Ploy MC, Da Re S. The stringent response promotes antibiotic resistance dissemination by regulating integron integrase expression in biofilms. MBio 2016;7(4).
[70] Shippy DC, Fadl AA. tRNA modification enzymes GidA and MnmE: potential role in virulence of bacterial pathogens. Int J Mol Sci 2014;15(10):18267–80.
[71] Shepherd J, Ibba M. Bacterial transfer RNAs. FEMS Microbiol Rev 2015;39(3): 280–300.
[72] Casilag F, Lorenz A, Krueger J, Klawonn F, Weiss S, Häussler S. The LasB elastase of *Pseudomonas aeruginosa* acts in concert with alkaline protease AprA to prevent flagellin-mediated immune recognition. Infect Immun 2016;84(1):162–71.
[73] Kayama S, Murakami K, Ono T, Ushimaru M, Yamamoto A, Hirota K, Miyake Y. The role of rpoS gene and quorum-sensing system in ofloxacin tolerance in *Pseudomonas aeruginosa*. FEMS Microbiol Lett 2009;298(2):184–92.
[74] Whiteley M, Parsek MR, Greenberg EP. Regulation of quorum sensing by RpoS in *Pseudomonas aeruginosa*. J Bacteriol 2000;182(15):4356–60.
[75] Schuster M, Lostroh CP, Ogi T, Greenberg EP. Identification, timing, and signal specificity of *Pseudomonas aeruginosa* quorum-controlled genes: a transcriptome analysis. J Bacteriol 2003;185(7):2066–79.
[76] Moscoso JA, Mikkelsen H, Heeb S, Williams P, Filloux A. The *Pseudomonas aeruginosa* sensor RetS switches type III and type VI secretion via c-di-GMP signalling. Environ Microbiol 2011;13(12):3128–38.
[77] Goodman AL, Merighi M, Hyodo M, Ventre I, Filloux A, Lory S. Direct interaction between sensor kinase proteins mediates acute and chronic disease phenotypes in a bacterial pathogen. Genes Dev 2009;23(2):249–59.
[78] Coggan KA, Wolfgang MC. Global regulatory pathways and cross-talk control *Pseudomonas aeruginosa* environmental lifestyle and virulence phenotype. Curr Issues Mol Biol 2012;14(2):47–70.
[79] Whitaker WB, Richards GP, Boyd EF. Loss of sigma factor RpoN increases intestinal colonization of *Vibrio parahaemolyticus* in an adult mouse model. Infect Immun 2014;82(2):544–56.